SALAMANDRA **61**(4): 423–441
30 October 2025 | ISSN 0036–3375

SALAMANDRA
German Journal of Herpetology

New insights into the diversity of *Oreobates* frogs (Anura: Craugastoridae): description of a new species from the Peruvian Yungas and comments on *O. quixensis* and *O. saxatilis*

Ernesto Castillo-Urbina[1,2], Miguel Vences[3], Mathias Dezetter[4], Frank Glaw[6], Christine Burgos[2], Lucia Aliaga[2], Grecia Torres-Ccasani[1,2], Sydney F. Hope[4,5], Alejandro Mendoza[1,2] & Jörn Köhler[7]

[1] Universidad Nacional Mayor de San Marcos, Museo de Historia Natural (MUSM), Departamento de Herpetología, Av. Arenales 1256, Lima 11, Peru

[2] Asociación Ararankha: Ecología y Conservación, Lima, Peru

[3] Zoological Institute, Technische Universität Braunschweig, Mendelssohnstr. 4, 38106 Braunschweig, Germany

[4] Association Nature Conserv'Action, Montpellier 34430, France

[5] Department of Psychology, Hunter College, City University of New York, 695 Park Avenue, New York, NY 10065, USA

[6] Zoologische Staatssammlung München (ZSM-SNSB), Münchhausenstr. 21, 81247 München, Germany

[7] Hessisches Landesmuseum Darmstadt, Friedensplatz 1, 64283 Darmstadt, Germany

Corresponding author: Jörn Köhler, ORCID 0000-0002-5250-2542,
e-mail: joern.koehler@hlmd.de

Manuscript received: 27 May 2025
Accepted: 1 August 2025 by Stefan Lötters

Abstract. We investigate the taxonomic status of specimens of the pristimantine frog genus *Oreobates* recently collected in montane rainforest within the Biocorredor Bosques de Vaquero 'Shunku Sacha', San Martín Department, Peru. A phylogenetic analysis of these frogs based on DNA sequences of the mitochondrial 16S rRNA gene revealed a lineage closely related to *Oreobates colanensis*. However, that lineage is divergent from *O. colanensis* by 10.1% uncorrected pairwise distance in the 16S gene fragment, and from other species of *Oreobates* included in the analysis by more than 13.8%. Moreover, specimens in that lineage are distinguished from those of all recognized nominal species of *Oreobates* by a unique combination of morphological characters, including skin on the dorsum granular, absence of dorsolateral folds, presence of nuptial pads in males, absence of vocal slits and vocal sacs in males, and the absence of basal webbing on toes. Consequently, we describe this lineage as a new species, *Oreobates shunkusacha* sp. n. We also report on additional vouchers of *Oreobates* collected in the lowland Amazonian rainforest of Panguana, Huánuco Department, central Peru. Based on morphology, mitochondrial (16S) and nuclear genes (POMC, RAG-1), we demonstrate that *Oreobates* specimens from this locality belong to two distinct species-level lineages, referred to as *O. quixensis* and *O. saxatilis*, thus providing conclusive evidence for sympatric occurrence of these two nominal taxa that were previously considered to have parapatric ranges. Furthermore, we provide and discuss data suggesting that a misidentification of previously sequenced specimens, including the paratopotype of *O. saxatilis*, is likely responsible for the paraphyly of *O. quixensis* and *O. saxatilis* in previously published mitochondrial trees. Upon correction of these putative misidentifications, the morphologically diagnosable species *O. quixensis* and *O. saxatilis* are monophyletic and occur in close sympatry at certain localities in the upper Amazon basin.

Key words. Amphibia, Pristimantinae, molecular genetics, morphology, Peru, sympatry, systematics, taxonomy, misidentification, conservation.

Introduction

The genus *Oreobates* Jiménez de la Espada, 1872 comprises a group of Neotropical frogs with assumed direct development which are distributed from southern Colombia to northern Argentina, with most species occurring along the eastern slopes of the Andes, reaching elevations of up to 3850 m a.s.l. (Padial et al. 2012, Montero-Mendieta et al. 2021). These frogs inhabit a variety of ecosystems, including humid Amazonian lowland, semi-deciduous forests, montane humid and dry forests, as well as high elevation Puna grasslands (Padial et al. 2008, 2012). Currently, *Oreobates* includes 26 described species (Frost 2025) but, despite recent taxonomic progress, species diversity re-

mains incompletely known. Candidate species have been identified by molecular data, including populations from Bolivia and Peru (Padial et al. 2012, Köhler & Padial 2016), and await formal taxonomic study. Given the suggested high rate of speciation of the genus particularly in the Yungas montane forests, which remain underexplored and partly difficult to access, and the comparatively low number of specimens available for certain species in scientific collections, a comprehensive understanding of the genus' diversity, distribution and morphological variation is still lacking (Padial et al. 2012, Pansonato et al. 2020, Venegas et al. 2021). In addition, phylogenetic studies confirm that *Oreobates*, as currently defined, is monophyletic, but there are partly ambiguous results with respect to the most basal phylogenetic relationships within the genus (Padial et al. 2012, 2014, Montero-Mendieta et al. 2021, Venegas et al. 2021).

During fieldwork in Peru, we collected specimens of *Oreobates*. Among these is one putative new species from the Biocorredor Bosques de Vaquero 'Shunku Sacha' in San Martín Department, Peru, which includes the three Conservation Concessions (CC) Sacha Runa, Yaku Kawsanapa, and Cordillera de Vaquero. It is an ecological corridor within the northern sector of the buffer zone of the Cordillera Azul National Park, connecting it to the southern margins of the Cordillera Escalera Regional Conservation Area. The Cordillera Azul is a mid-elevation mountain ridge (< 2350 m a.s.l.) limited by the Huallaga river basin to the west, and by the Ucayali river basin to the east. The physiography of this ridge, with basimontane forest surrounding areas of Yungas mountain forest, appears to have led to the diversification of unique and endemic frog species (e.g., Myers & Daly 1979, Flores & McDiarmid 1989, Lötters et al. 1997, 2002, Lötters 2003, Brown & Twomey 2009). Recent taxonomic studies have revealed new species or re-discoveries of anurans that are currently considered to be endemic to the Cordillera Azul (Cusi et al. 2017, Castillo-Urbina et al. 2021, 2023, Köhler et al. 2022) but over all this mountain range remains little explored. The same is true for the Cordillera Escalera (< 2220 m a.s.l.), with most knowledge on amphibians from this area being limited to the southernmost portion of this mountain ridge (e.g., Duellman & Schulte 1993, Twomey et al. 2014, Cusi et al. 2020).

We also collected *Oreobates* specimens in the Amazonian lowlands of central Peru. Specimens from this region are recovered as one lowland clade encompassing the species *O. quixensis* and *O. saxatilis*. Even though *O. quixensis* and *O. saxatilis* are reciprocally diagnosable morphologically, they were recovered as paraphyletic based on mitochondrial DNA phylogenetic analyses, which constitutes a taxonomic challenge (Padial et al. 2012). Recent molecular population structure analyses showed the data for samples of *O. quixensis* and *O. saxatilis* were mostly consistent with the presence of two clusters, but the clusters did not fully correspond to respective species identifications (Montero-Mendieta et al. 2021). Potential explanations included incomplete lineage sorting, misidentifications of voucher specimens and ongoing genetic flow between the two species (Padial et al. 2012, Montero-Mendieta et al. 2021).

In this study, we investigate the taxonomic status of the *Oreobates* population discovered in the montane forest of the CCs Sacha Runa and Yaku Kawsanapa in the San Martín Department, provide evidence for its specific distinctness from all known species of *Oreobates*, and describe it as a new species. In addition, we provide new data for the lowland species *O. quixensis* and *O. saxatilis* and discuss the implications for their phylogenetic relationships and distribution.

Materials and methods

Fieldwork and voucher specimens

Fieldwork was conducted in October 2022 and in March 2025 in different areas of the Biocorredor Bosques de Vaquero 'Shunku Sacha', San Martín Department, Peru, including the Conservation Concession (CC) Sacha Runa and the CC Yaku Kawsanapa, in collaboration with the community-based associations managing the two CCs, namely AESARUSA, and ABAFYK (see Shanee et al. 2015, 2020 for overviews about CCs in San Martín Department), and during multiple expeditions between 2008 and 2019 at the Area de Conservación Privada Panguana, Huánuco Department, central Peru. Specimens were observed and collected during opportunistic surveys at night and day. Geographical coordinates were recorded using handheld GPS receivers set to WGS84 datum. In March 2025, we also opportunistically recorded the field-active body temperature of individuals, as well as substrate and air temperatures at the exact location where each individual was found, using an infrared thermometer (Fluke 62 Max). Collected specimens were euthanized with an overdose of 5% lidocaine or benzocaine gel applied on the ventral surfaces of individuals (McDiarmid 1994). Tissue samples were taken prior to fixation and stored in 99% ethanol, while specimens were fixed using 96% ethanol or formalin and subsequently stored in 70% ethanol. Specimens were deposited in the herpetological collection of the Museo de Historia Natural, Universidad Nacional Mayor de San Marcos (MUSM), Lima, Peru, and Zoologische Staatssammlung München (ZSM), Germany. All additional museum abbreviations used follow those of Frost (2025). FGZC refers to Frank Glaw field numbers.

Morphology

Morphological measurements (in millimeters) were taken to the nearest 0.1 mm by the first author using a digital caliper, with the aid of a stereoscopic microscope. For proper comparison, the definition of morphological character states follows those established by Duellman & Lehr (2009) and the diagnostic and descriptive schemes follow those of Padial et al. (2012). The measurements taken and

used throughout the text are as follows: SVL (snout–vent length), HL (head length; straight-line distance from the posterior corner of the mouth to the tip of the snout), HW (head width; measured at the level of the jaw angle), TD (tympanum diameter; measured horizontally), IND (internarial distance), IOD (interorbital distance; between the anterior margins of the orbits), ED (horizontal eye diameter), EW (upper eyelid width), END (eye–nostril distance; from the anterior margin of the orbit to the center of the nostril), HaL (hand length; from the proximal edge of the inner metacarpal tubercle to the tip of the third finger), TL (tibia length; from the femur–tibia articulation to the tibia–heel proximal articulation), THL (thigh length; from the middle of the cloacal slit to the proximal part of the femur–tibia articulation), and FL (foot length; distance from the proximal margin of the inner metatarsal tubercle to the tip of toe IV). Color in life is described based on digital photographs.

Molecular genetics

First, our molecular genetic analysis primarily aimed at the identification of lineage divergence among focal samples of *Oreobates* using the mitochondrial 16S rRNA (16S) gene. For representative taxon sampling, we used BLAST searches (Altschul et al. 1990) of newly generated 16S sequences of the *Oreobates* samples from Shunku Sacha against the GenBank nucleotide archive and downloaded a selection of sequences of representatives of all nominal species (and few candidate species) of *Oreobates* (sensu Venegas et al. 2021), with *O. zongoensis* being the only nominal species for which 16S sequence data are not available. Two species of *Lynchius* (*L. simmonsi, L. waynehollomonae*), the sister group of *Oreobates* (Pyron & Wiens 2011, Motta et al. 2016), were added to the sampling as outgroup taxa. Second, as our first analysis unexpectedly indicated the presence of two species-level lineages at Panguana, we performed the same analysis again by now adding all 16S sequences available from GenBank for the two nominal species *O. quixensis* and *O. saxatilis*, plus sequences from all *Oreobates* specimens collected by us at Panguana. To assess potential admixture between the two distinct *Oreobates* lineages occurring at Panguana, we furthermore sequenced the nuclear-encoded genes POMC and RAG-1 of these samples.

DNA was extracted using a standard salt extraction protocol. Fragments of the mitochondrial gene for 16S rRNA (16S) and the nuclear-encoded gene for pro-opiomelanocortin (POMC) and the recombination-activating gene 1 (RAG-1) were amplified in polymerase chain reactions (PCR) with the following primers and cycling conditions: 16S: primers 16SAr-L (5'-CGCCTGTTTATCAAAAACAT-3') and 16SBr-H (5'-CCGGTCTGAACTCAGATCACGT-3') (Palumbi et al. 1991), cycling conditions 94 °C (60 sec), 33 cycles of 95 °C (45 sec), 55 °C (45 sec), 72 °C (90 sec), and final elongation at 72 °C (600 sec); POMC: primers POMC-DRVF1 (5'-ATATGTCATGASCCAYTTYCGCTGGAA-3') and POMC-DRVR1 (5'-GGCRTTYTTGAAWAGAGTCATTAGWGG-3') from Vieites et al. (2007), cycling conditions 95 °C (120 sec), 40 cycles of 95 °C (45 sec), 47 °C (45 sec), 72 °C (60 sec), and final elongation at 72 °C (600 sec); RAG-1: two pairs of primers were successively used in a nested PCR approach, first PCR with primer pair Rag1-Mart-F1 (5'-AGCTGGAGYCARTAYCAYAARATG-3') and Rag-1Mart-R6 (5'-GTGTAGAGCCARTGRTGYTT-3'), modified from Martin (1999), second PCR with primers Rag-1-AmpF2 (5'-ACNGGNMGICARATCTTYCARCC-3') and Rag1-UC-R (5'-TTGGACTGCCTGGCATTCAT-3') from Chiari et al. (2004) and Rakotoarison et al. (2015), both PCRs with cycling protocol 94 °C (240 sec), 45 cycles of 94 °C (45 sec), 45 °C (40 sec), 72 °C (120 sec), and final elongation at 72 °C (600 sec). PCR products were resolved on automated DNA sequencers by LGC Genomics (Berlin, Germany). All new DNA sequences were submitted to GenBank (accession numbers PX131115–PX131127 and PX125881–PX125892). 16S sequences were combined with those from other studies downloaded from GenBank. A full table with all sequences used, their accession numbers and metadata is available from the Zenodo repository (https://doi.org/10.5281/zenodo.16876682).

To estimate evolutionary relationships within *Oreobates*, we used a Maximum Likelihood (ML) phylogenetic approach on the 16S alignment. Sequences were exported to AliView v1.26 (Larsson 2014), edited, and aligned using MAFFT v7.310 (Katoh & Standley 2013) with the L-INS-i parameter as the iterative refinement method (Katoh et al. 2005), resulting in an alignment of 588 base pairs. We employed the W-IQ-TREE web server (Trifinopoulos et al. 2016) to infer a molecular phylogeny under ML as the optimality criterion. The best evolutionary model was determined using ModelFinder under the Bayesian Information Criterion (BIC) implemented in IQ-TREE, identifying TIM2+F+I+G4 as the best-fitting substitution model for the dataset (-m TEST command; Kalyaanamoorthy et al. 2017). To evaluate branch support, ultrafast bootstrap values were obtained from 2000 pseudoreplicates and 10,000 iterations as the maximum number to stop (-bb 2000 and -nm 10,000 commands in IQ-TREE). Additionally, the Shimodaira-Hasegawa approximate likelihood ratio test (SH-aLRT) was performed with 1000 replicates (-alrt 1000 command; Shimodaira & Hasegawa 1999, Guindon et al. 2010). Genetic divergences were quantified as uncorrected pairwise distances (p-distances) using pairwise alignments in MEGA v11 (Tamura et al. 2021) with default settings (pairwise deletion).

For the Panguana samples, the alignments of the nuclear-encoded POMC and RAG-1 gene fragments (430 and 1328 bp, respectively) were analyzed independently from the mitochondrial sequences to understand concordance (or absence thereof) in their differentiation. We used a genealogy visualization approach to graphically represent the relationship among alleles (haplotypes). Haplotypes were estimated with the PHASE algorithm (Stephens et al. 2001), and haplotype genealogies estimated with the Fitch tree algorithm (Salzburger et al. 2011, Matschiner 2016) in Hapsolutely (part of iTaxoTools) (Vences et al. 2021, 2024).

Threat status

We assessed the Red List status of the species according to the IUCN Red List criteria (IUCN 2001). Given the habitats and elevations where we observed *Oreobates* from CCs Sacha Runa and Yaku Kawsanapa, we estimated its geographic range by calculating the area within the Biocorredor Bosques de Vaquero mountain ranges at elevations higher than 1350 m a.s.l. using QGIS software version 3.42.1.

Nomenclatural acts

The electronic edition of this article conforms to the requirements of the amended International Code of Zoological Nomenclature, and hence the new name contained herein is available under that Code from the electronic edition of this article. This published work and the nomenclatural acts it contains have been registered in ZooBank, the online registration system for the ICZN. The LSID (Life Science Identifier) for this publication is: urn:lsid:zoobank.org:pub:7C33D393-DC77-4C6C-8189-218DDF20C180. The electronic edition of this work was published in a journal with an ISSN, and has been archived and is available from the following digital repositories: zenodo.org, salamandrajournal.com.

Results

Identity of *Oreobates* populations from Shunku Sacha

Our Maximum Likelihood tree (Fig. 1) recovered *Oreobates* monophyletic with high support (bootstrap/ SH-aLRT values = 100/100). The tree topology is generally in agreement with those published previously (Padial et al. 2012, Köhler & Padial 2016, Pansonato et al. 2020, Venegas et al. 2021), except for some ambiguous relationships receiving no support (*O. amarakaeri, O. lundbergi*) and most basal nodes receiving only low to moderate support. The three samples of the population from Shunku Sacha are recovered monophyletic and sister to *O. colanensis* with high support (99/99).

Uncorrected pairwise distances in the 16S gene fragment of the samples from Shunku Sacha to *O. colanensis* amount to 10.1%, and range between 13.8–21.4% to all other known species of *Oreobates* included in the analysis.

Morphological examination of the Shunku Sacha specimens and comparison with museum vouchers revealed that they exhibit a combination of external characters that distinguish them from all currently recognized nominal species of *Oreobates* (see below). Consequently, with these three independent lines of evidence (phylogenetic relationships, high mitochondrial divergence and morphological distinctness), we regard that population a distinct evolutionary lineage and describe it as a new species.

Taxonomy

***Oreobates shunkusacha* sp. n.**

ZooBank LSID: urn:lsid:zoobank.org:act:FF57198D-C042-4097-9ED9-9415826B9314

Holotype: MUSM 41865, adult female (Figs 2–3), from Conservation Concession Sacha Runa (-6.713915, -76.109471, 1496 m a.s.l.), Sauce District, San Martín Province, San Martín Department, Peru, collected on 28 October 2022 (21:34 h) by L. Aliaga, C. Burgos, S. F. Hope, and M. Dezetter.

Paratypes: MUSM 41863–41864, two adult males, from CC Sacha Runa (-6.715414, -76.103853 and -6.714223, -76.10752, at 1596 and 1540 m a.s.l., respectively), collected on 28 October 2022 (between 19:31 to 20:47 h) by L. Aliaga, C. Burgos, S. F. Hope, and M. Dezetter; MUSM 42182, one adult female, and MUSM 42183–42184, two adult males, from CC Sacha Runa (-6.71545, -76.10317, 1600 m a.s.l.), MUSM 42185, one adult female, from CC Sacha Runa (-6.71488, -76.10691, 1552 m a.s.l.), collected between 19 and 22 March 2025 (between 19:50 to 22:16 h) by C. Burgos, E. Castillo-Urbina, M. Fernandez, M. Valle, T. Vasquez, and M. Dezetter. All localities in Sauce District, San Martín Province, San Martín Department, Peru.

Referred specimens: MUSM 42186, 42188–42189, three adult males, from CC Yaku Kawsanapa (-6.64827, -76.16221, 1414 m a.s.l.) and MUSM 42187, one adult male, from CC Yaku Kawsanapa (-6.64734, -76.16152, 1351 m a.s.l.) Chazuta District, San Martín Province, San Martín Department, Peru, collected on 12 March 2025 (between 19:10 to 20:20 h) by C. Burgos, E. Castillo-Urbina, M. Fernandez, M. Valle, T. Vasquez, and M. Dezetter.

Definition: A moderately robust species of *Oreobates* (SVL of adult males 24.4–26.4 mm, n = 8; adult females SVL 37.9–41.8 mm, n = 3), defined by the following combination of characters: (1) skin of dorsum granular, granules small, round to subconical, homogeneous in size; a thin vertebral fold present; dorsolateral folds absent; venter smooth; posterior surfaces of thighs areolate, skin in groin smooth; discoidal fold present; postrictal tubercles present, rounded; (2) tympanic membrane distinct, large, about 40–54% of eye diameter; anterior part of tympanic annulus distinct; supratympanic fold present, well-defined, concealing the upper part of the tympanic annulus; (3) head slightly longer than wide to nearly as long as wide (HW/HL = 0.88–0.99); snout long, rounded in dorsal view and in lateral profile; canthus rostralis sinuous in dorsal view, rounded in cross-section; (4) cranial crests absent; upper eyelid bearing small, scattered, subconical tubercles, being slightly larger than dorsal tubercles; (5) dentigerous process of vomers large, prominent, oval in shape, situated posteromedial to choanae (posterior margin at level of choanae), their width about 1.6 times the diameter of choanae, bearing 5 to 6 vomerine teeth; (6) males without

vocal slits and vocal sacs; (7) hands with long and slender fingers, first finger slightly longer than second; subarticular tubercles large and prominent, conical; supernumerary tubercles prominent, round, smaller than subarticular tubercles; fingertips round, barely enlarged, lacking circumferential grooves; lateral fringes on fingers present, weak; nuptial pads present on males, dorsally and medially on Finger I; (8) antebrachial and ulnar tubercles present, low and minute, 1–3 ulnar tubercles; (9) heel and outer side of tarsus bearing very low subconical tubercles, being slightly larger than tubercles on dorsal surfaces of thighs; (10) inner metatarsal tubercle ovate, prominent; outer metatarsal tubercle smaller than the inner metatarsal tubercle, subconical, prominent; subarticular tubercles conical, prominent; supernumerary tubercles smaller than subarticular tubercles, prominent, round; (11) toes long and slender, lateral fringes present and weak, webbing absent; toe V and III equal in length, reaching to the middle of second

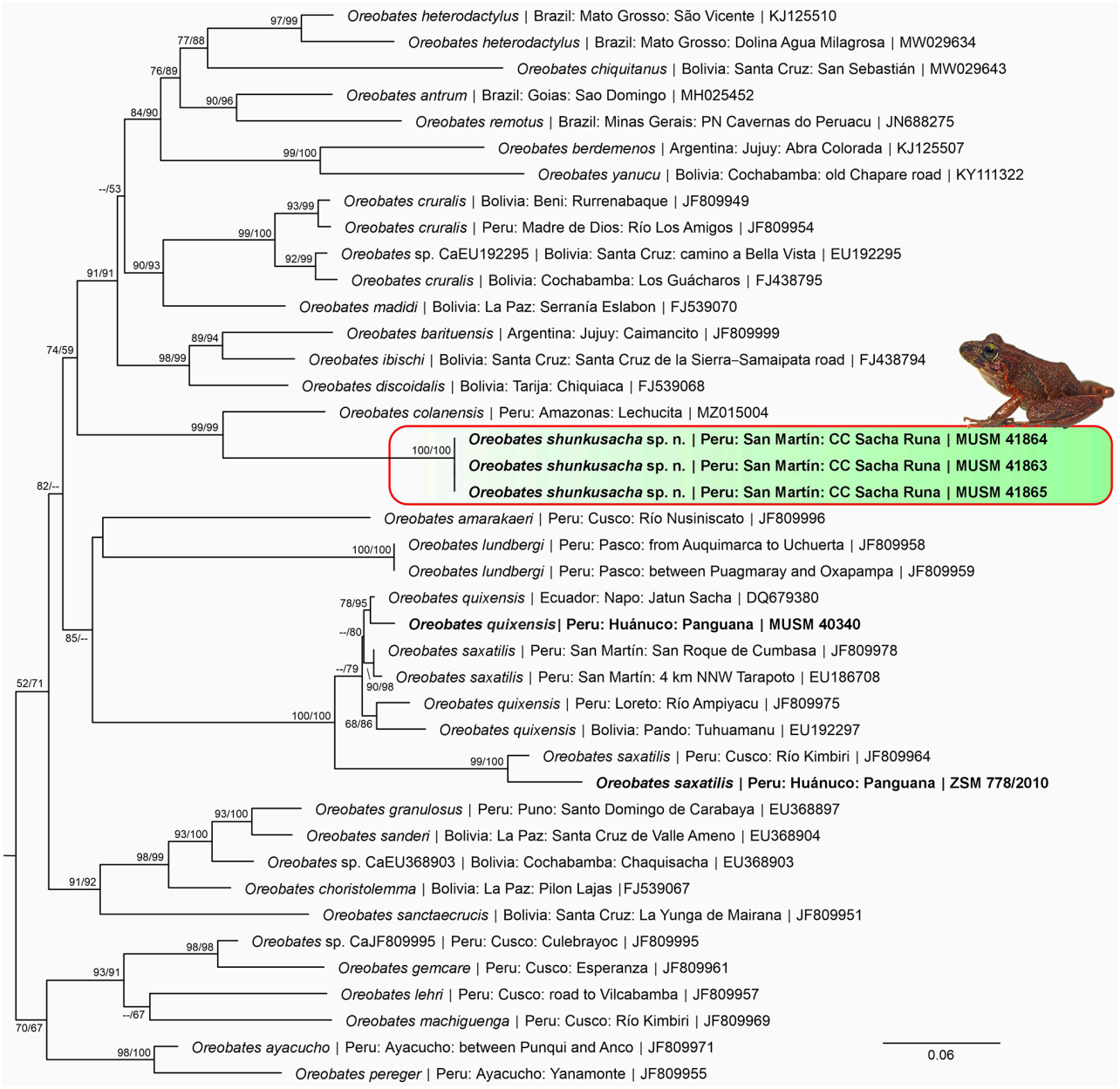

Figure 1. Maximum Likelihood phylogenetic tree of samples of *Oreobates*, inferred from an alignment of the mitochondrial 16S rRNA gene. Numbers at nodes are rounded bootstrap values in percent (2000 pseudoreplicates; not shown if < 50%), followed by SH-aLRT values (1000 replicates; not shown if < 50) as calculated with IQ-TREE. The taxon name is followed by sample locality and GenBank accession number, or voucher number for newly produced sequences (terminals in bold font). Two samples of *Lynchius* were used to root the tree (not shown for better graphical presentation). Inset photo depicts the holotype of *O. shunkusacha* sp. n. (MUSM 41865) in life.

subarticular tubercle of Toe IV; tips of toes slightly enlarged, rounded, lacking circumferential groove or ungual flap on toe I, tips of toes II, III, IV, and V bearing distinct ungual flaps; foot length 49.8–57.8% of SVL; (12) axillary glands absent.

Diagnosis: *Oreobates shunkusacha* differs from all other known species of *Oreobates* by the unique combination of skin on dorsum granular with granules being small, round to subconical and homogeneous in size, absence of dorsolateral folds, presence of nuptial pads in males, absence of vocal slits and vocal sacs in males, and the absence of basal webbing on toes.

In external morphology, *O. shunkusacha* superficially resembles *O. lehri*, *O. zongoensis*, and *O. machiguenga* in having a granular dorsal skin texture, with granules being homogeneous in size and in the absence of dorsolateral folds. It mainly differs from *O. lehri* and *O. zongoensis* (characters in parentheses) in having nuptial pads in males (absent), and males lacking vocal slits (present). Furthermore, it differs from *O. lehri* by having the first finger slightly longer than second (finger I shorter than finger II), supernumerary tubercles on feet present, distinct and subconical (absent), and the absence of axillary glands (present). Additionally, it can be distinguished from *O. zongoensis* by supernumerary tubercles on plantar surfaces being distinct and subconical (indistinct), tips on toes slightly enlarged, rounded (slightly enlarged, truncated), lateral fringes on toes present and weak (absent), dorsal color pattern in life with pale chevron-shaped marking (uniformly dark brown, markings absent), ventral surfaces with some dark mottling (uniformly pinkish-brown), and a golden iris in life (bright copper-red). The new species can be distinguished from *O. machiguenga* in having a dis-

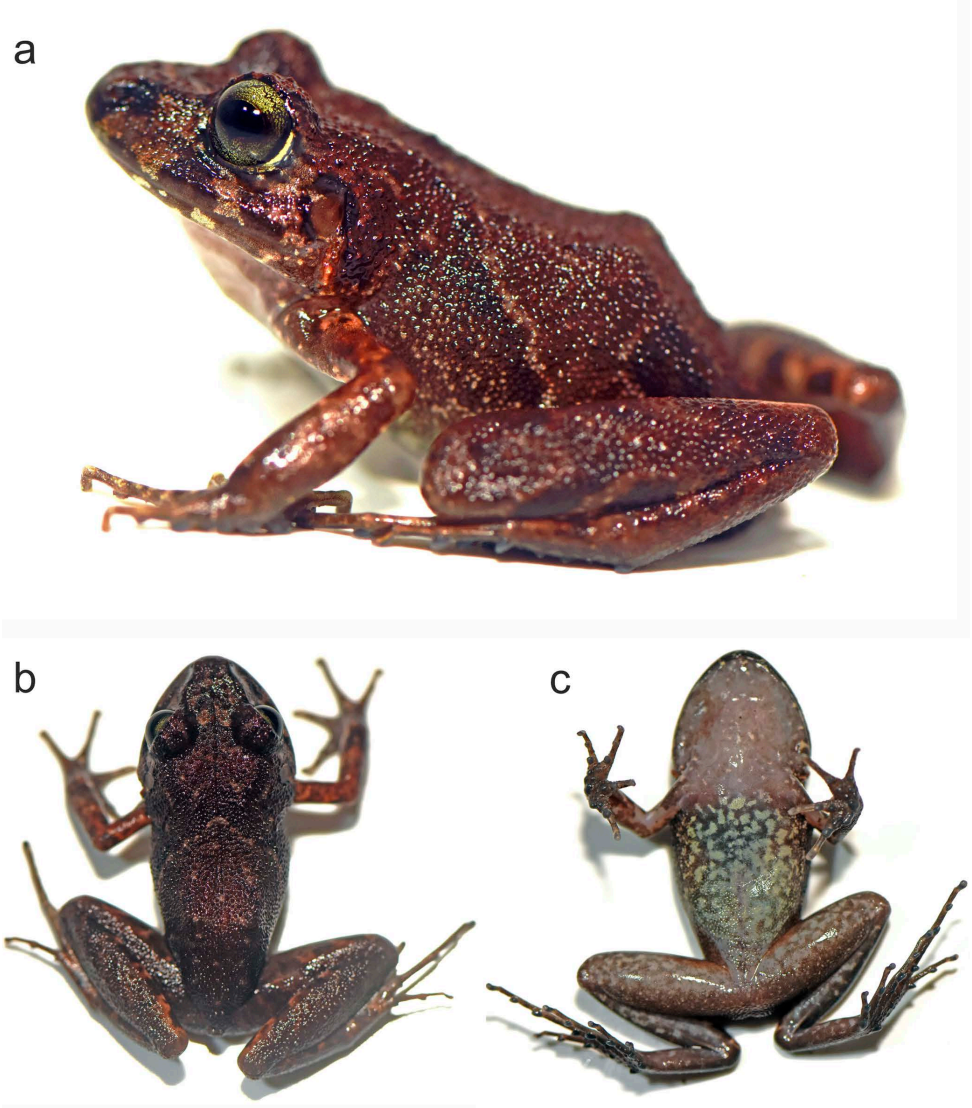

Figure 2. Adult female holotype of *Oreobates shunkusacha* sp. n. (MUSM 41865) in life (SVL 37.9 mm): (a) lateral, (b) dorsal and (c) ventral views. Not to scale.

tinct supratympanic fold (absent), canthus rostralis sinuous in dorsal view (convex), dentigerous processes of vomers oval in shape (triangular), snout long (short), and webbing on toes absent (present, basal between toe III and toe IV).

The new species may occur in geographical proximity to other species of *Oreobates* (i.e., *O. saxatilis*, *O. quixensis*, *O. lundbergi*). It differs mainly from all these by having skin of dorsum granular, with granules being small and homogeneous in size (finely tuberculate with distinctly larger scattered tubercles in *O. saxatilis*, tuberculate with many large subconical tubercles in *O. quixensis*, and smooth with small scattered tubercles in *O. lundbergi*). Furthermore, *O. shunkusacha* differs from *O. saxatilis* and *O. quixensis* by having nuptial pads in males (absent).

Oreobates shunkusacha is most closely related to *O. colanensis* and mainly differs from it by the absence of dorsolateral folds (present, distinct), the presence of nuptial pads in males (absent), the absence of contrasting color pattern on the hidden surfaces of body, as axilla, groins, anterior and posterior surfaces of thighs, and shank (present, white or cream blotches on a dark brown background), and belly pale with faint brown marks to dark brown mottling (belly dark brown suffused with red with numerous white flecks).

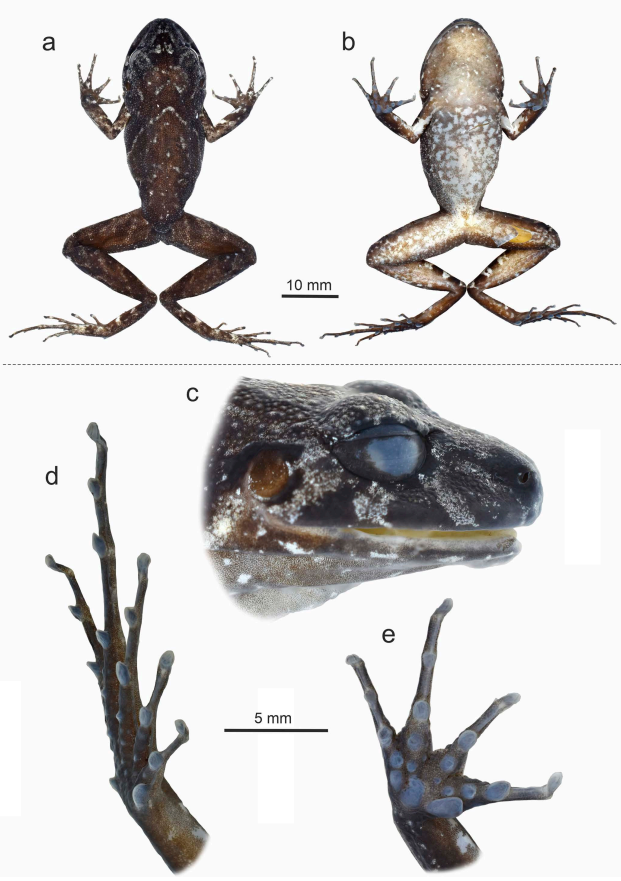

Figure 3. Preserved female holotype of *Oreobates shunkusacha* sp. n. (MUSM 41865): (a) dorsal and (b) ventral views; (c) lateral view of the head; (d) plantar surface of right foot; and (e) palmar surface of right hand.

Holotype description: Adult female (Figs 2–3). Head slightly wider than body, head longer than wide (HW/HL = 0.93); snout long, rounded in dorsal view and in lateral profile (Fig. 3c); nostrils slightly protuberant, oriented laterally; canthus rostralis slightly sinuous in dorsal view, rounded in cross-section; loreal region slightly concave, sloping gradually to the lips; lips not flared; upper eyelid with numerous, small, subconical granules; cranial crests absent. Supratympanic fold short, extending to anterior level of insertion of arm and to the inferior level of the end of the tympanum, concealing the upper part of the annulus posteriorly; tympanic membrane distinct, anterior part of tympanic annulus distinct; tympanic membrane nearly round, transparent, its diameter slightly less than half of eye diameter; postrictal tubercles present, round. Choanae not concealed by palatal shelf of the maxillary arch when roof of mouth is viewed from below; choanae medium in size, round, separated by a distance equal to five times the diameter of choana; dentigerous processes of the vomers prominent, oblique, oval, situated posteromedial to choanae (posterior margin at level of choanae), their width about 1.6 times the diameter of choanae, bearing 5–6 vomerine teeth. Skin on dorsum and flanks granular, with small, low, round granules, homogeneous in size, covering the entire dorsum; ventral surfaces smooth; thighs coarsely areolate posteriorly; occipital fold V-shaped; dorsum bearing one thin vertebral fold, hardly recognizable, form the tip of the snout to the pelvic region; dorsolateral fold absent; discoidal fold present, weak; thoracic fold present, distinct; skin in groin areolate. Antebrachial tubercle and three ulnar tubercles present, low and minute; palmar tubercle divided in two subunits, inner irregular in form larger than outer oval; thenar tubercle prominent, triangular in outline; supernumerary tubercles prominent; subarticular tubercles rounded, larger than supernumerary tubercles; finger tips narrowly rounded; pads absent, circumferential grooves and ungual flaps absent; fingers lacking lateral fringes and webbing; relative length of fingers: I > II < III > IV (Fig. 3e). Toes long and slender, foot length 52% of SVL; heel and outer side of tarsus bearing very low conical tubercles, tarsus lacking folds; inner metatarsal tubercle oval, prominent, larger than outer metatarsal tubercle; outer metatarsal tubercle conical, prominent; plantar supernumerary tubercles present, distinct, subconical; subarticular tubercles prominent, conical; toes with weak lateral fringes proximally; toe webbing absent; toe tips rounded, barely expanded, without circumferential groove or ungual flap on toe I; tips of toes II, III, IV, and V each bearing distinct ungual flap; relative length of toes: I < II < III > V < IV (Fig. 3d). Toe V and Toe III reaching to the middle of second subarticular tubercle of Toe IV.

Measurements (in mm): SVL 37.9; TL 19.7; FL 19.3; HL 15.2; HW 14.1; ED 4.2; TY 1.8; IOD 3.3; EW 3.5; IND 3.3; E–N 4.8.

Table 1. Morphological measurements (in mm) and proportions of specimens of *Oreobates shunkusacha* sp. n. (see text for abbreviations). ** = holotype; * = paratype.

MUSM	41865**	42182*	42185*	41864*	41863*	42183*	42184*	42186	42187	42188	42189
sex	female	female	female	male	male	male	male	male	male	male	male
SVL	37.9	41.8	38.8	24.7	26.3	26.4	24.6	24.7	24.4	24.5	25.2
TL	19.7	21.2	20.5	13.8	14.3	13.5	13.3	13.4	12.7	13.5	13.8
FL	19.3	21.3	21.0	13.7	14.1	13.6	13.7	13.3	12.1	14.1	12.6
HL	15.2	17.1	15.8	10.4	10.6	11.2	10.9	10.2	10.0	10.4	10.6
HW	14.1	16.0	15.6	9.1	9.3	10.3	9.7	10.1	8.7	9.6	10.0
ED	4.2	5.2	5.8	3.3	3.5	3.5	3.8	3.7	3.7	3.8	3.9
IOD	3.3	4.2	3.6	2.4	2.5	2.6	2.2	2.5	2.3	2.6	2.4
EW	3.5	3.7	3.1	2.4	2.5	2.2	2.3	2.2	2.1	2.4	2.2
IND	3.3	4.1	3.5	2.6	2.5	2.8	2.6	2.6	2.3	2.4	2.3
E-N	4.8	5.3	4.8	3.0	3.0	3.2	3.1	3.1	3.0	3.1	3.2
TY	1.8	2.3	2.3	1.6	1.6	1.9	1.7	1.7	1.5	1.8	1.6
TL/SVL	0.52	0.51	0.53	0.56	0.54	0.51	0.54	0.54	0.52	0.55	0.55
HL/SVL	0.40	0.41	0.41	0.42	0.40	0.42	0.44	0.41	0.41	0.42	0.42
HW/HL	0.93	0.94	0.98	0.88	0.88	0.91	0.89	0.99	0.87	0.92	0.94
TY/ED	0.43	0.44	0.40	0.48	0.46	0.54	0.45	0.45	0.41	0.47	0.41

In life (Fig. 2), dorsal surfaces dark-brown with a narrow pale chevron that extents onto the flanks; snout paler brown compared to dorsum; canthal stripe absent; two pale labial bars, irregular, narrow in width above and becoming wider below; lower jaw dark brown with some white speckles; supratympanic fold and anterior part of the annulus blackish; arms reddish brown with diffusely defined dark brown transverse bars; dorsal surfaces of hands brown with fine white markings; legs pale brown with diffusely defined dark-brown transverse bars, more clearly defined medially; dorsal surfaces of feet with well-defined dark-brown transverse bars. Ventrally, throat greyish with a pinkish tint, with few scattered white marks at the margin; brachial and antebrachial surface with a pale patch; chest, belly and ventral surface of forelimbs cream with dark brown mottling, palms and soles dark brown. Iris greenish-golden with black reticulation and a fine dark-brown circumpupillary line.

In 70% ethanol (Fig. 3), color pattern is the same as in life with dorsal surfaces brown, but top of head turned paler than the background color. Markings on head are darker than the dorsum; pale chevron-shaped marking on dorsum and labial bars more distinct than in life; flanks dark brown; forearms brownish cream (lacking the reddish color in life), legs pale brown with dark brown cross-bars with some pale edges. Ventral surfaces whitish-cream with gray mottling.

Variation: The studied females are larger in size compared to males. Body proportions are rather similar in all individuals. For variation in measurement and proportions see Table 1. All specimens have the skin on dorsum granular and with granules homogeneous in size, with the females having only few scattered slightly enlarged subconical granules, whereas in the males these slightly enlarged subconical granules are more numerous, especially on the posterior dorsum. The discoidal fold is weakly expressed in the females, whereas in the males the discoidal fold is distinct. The fine mid-dorsal fold starts at the anterior part of the snout, or in the scapular region, as in MUSM 41863 and 41864. The inner subunit of the palmar tubercle is irregular in shape in the holotype, but oval in all other specimens. Variation is also evident with respect to color pattern. Dorsal coloration varies from the presence of a pale chevron, irregular pale markings, as seen in MUSM 42182, or a lack of such pattern, as in MUSM 42187. Paratypes MUSM 41864 and 42183 exhibit faint pale dorsolateral stripes that begin at the posterior corner of the eye and extend to the lumbar region. In specimen MUSM 42189, the dorsolateral stripe is broader with blurred edges, and its pale coloration extends across the lumbar region. Female MUSM 42185 exhibits some large white blotches on the dorsal surface of the left hindlimb. Male MUSM 42186 has a thin light-brown vertebral line extending from the scapular region to the cloaca. Ventral coloration on belly ranges from cream with dark brown mottling to less contrasting mottling, as in MUSM 41864 and 42189, or pinkish cream with only faint mottling, as in MUSM 41863 and 42187 (Fig. 4).

Distribution and natural history: *Oreobates shunkusacha* is only known from two localities, the CC Sacha Runa, located in Sauce District, and the CC Yaku Kawsanapa, located in Chazuta District, San Martín Department, Peru, at elevations of 1351–1600 m a.s.l., in the Biocorredor Bosques de Vaquero 'Shunku Sacha', within the buffer zone of Parque Nacional Cordillera Azul (Fig. 5). CCs Sacha Runa and Yaku Kawsanapa comprise primary basimontane Yunga

forests that are bordered by patches of secondary forest, with deforested areas and agricultural plots nearby (Fig. 6). The individuals were found active during the night between 19:00 and 22:40 h, and were observed either on leaf litter or on moss, both on steep slopes and on plane relief within primary basimontane forest. Individuals were also observed a few meters from the mountain lake 'Cocha La Encantada', on the leaf litter within dense vegetation covered by moss and ferns (Fig. 6b). In March 2025, the mean field body temperature (± standard deviation) of active individuals was 18.3 ± 0.3 °C, while the mean substrate and air temperatures were 18.0 ± 0.5 °C and 21.3 ± 2.7 °C, respectively. Microhabitats consisted of dense forest undergrowth on rocky and sandy soil, covered by a thick layer of leaf litter and roots, near small surface and underground streams (Fig. 6c). These forest habitats are temporarily flooded during periods of heavy rain. Some individuals were observed retreating under tree roots and into complex hollow microhabitats. Gravid females were observed in March, with cream to yellow eggs visible through the skin on the posterior venter and flanks. In contrast, the female holotype collected in October was not gravid. Other anurans recorded in close sympatry with *O. shunkusacha* are *Dendropsophus* cf. *aperomeus*, *Scinax* cf. *pedromedinae*, *Pristimantis* sp. (*lacrimosus* group), *P.* sp. (*danae* group), *Chiasmocleis* cf. *tridactyla*, and *Rhinella* sp. (*festae* group). *Oreobates saxatilis* and *O. quixensis* occur at nearby sites at lower elevations (verified by preliminary 16S barcoding results). Calls remain unknown.

Conservation status: The buffer zone of the Cordillera Azul National Park is facing high deforestation rates associated with agricultural expansion and is the National Park buffer zone in San Martín that experienced the highest fragmentation rate between 2017 and 2021, with the number of forest patches increasing nearly fivefold (Chávez & Puerta 2024). Within the Biocorredor Bosques de Vaquero, CC Sacha Runa and CC Yaku Kawsanapa are facing significant deforestation threats associated with the expansion of agricultural land for coffee crops toward higher elevations (Fig. 6d, Supplementary Fig. S1). Even though these locally run, landscape-level Conservation Concession initiatives can provide effective solutions to deforestation, they currently lack access to support and economic resources (Shanee et al. 2015). All individuals were observed in undisturbed primary basimontane forest. Within the Biocorredor Bosques de Vaquero mountain range, we estimated a geographic range of 30.83 km² of basimontane Yunga

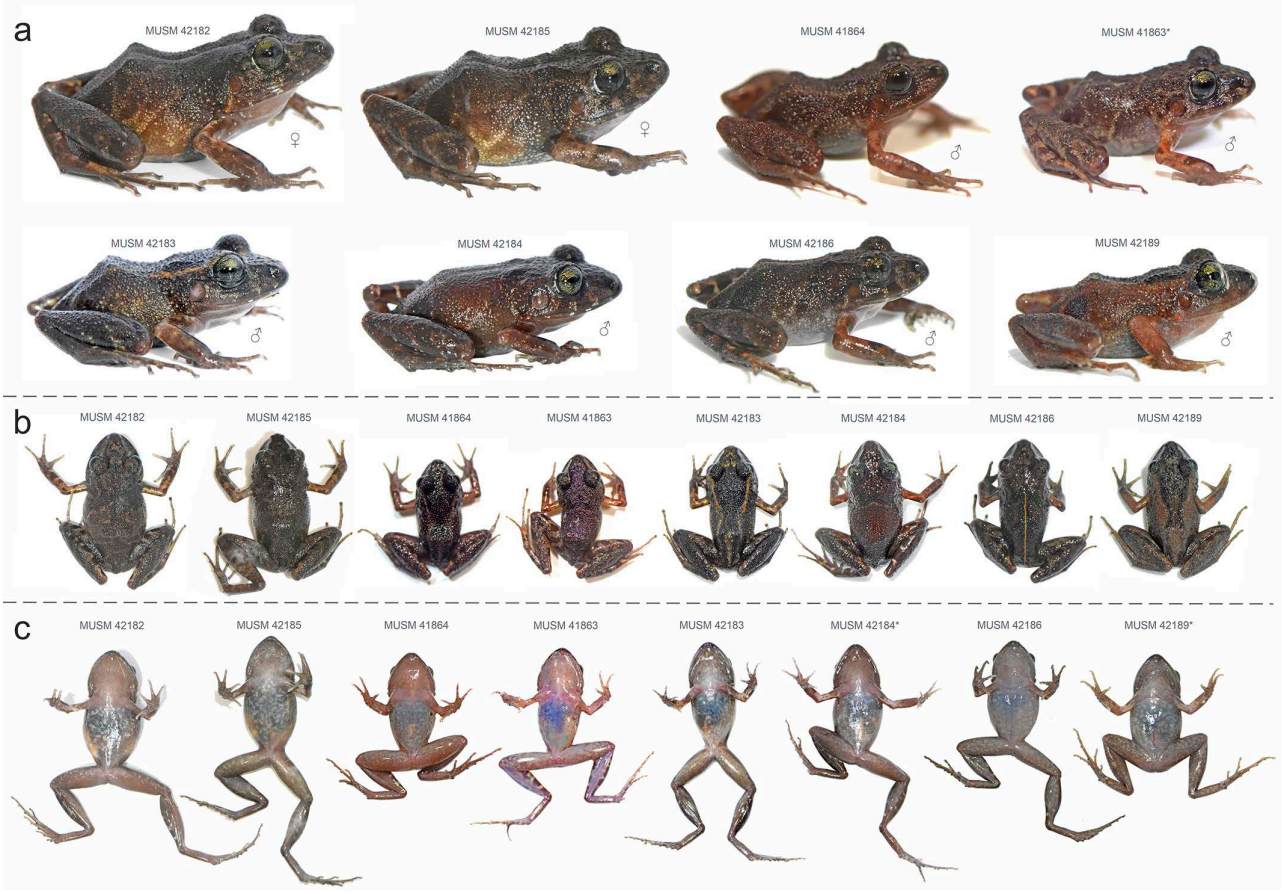

Figure 4. Photographs showing variation among specimens of *Oreobates shunkusacha* sp. n. in life in (a) lateral, (b) dorsal, and (c) ventral views (* = mirrored images). Not to scale.

forest where *O. shunkusacha* potentially occurs. Given its assumed distribution range of less than 500 km², the observed decline in its extent of occurrence and habitat quality due to deforestation, and the fact that it has fewer than five known threat-defined locations, we propose assigning *O. shunkusacha* to the Red List category Endangered (EN) B2a+b(iii).

Etymology: The species epithet refers to the type locality, Biocorredor Bosques de Vaquero 'Shunku Sacha', with 'shunku' meaning 'hearth' and 'sacha' meaning 'forest' in San Martín Kitchwa-Lamista language. It is treated as an invariable noun in apposition. As common names, we propose 'Shunku Sacha big-headed frog' in English language and 'Rana cabezona de Shunku Sacha' in Spanish language.

Sympatry of *O. quixensis* and *O. saxatilis*

While we conducted the phylogenetic analysis to evaluate the relationships and distinctness of the putative new species from Shunku Sacha, we also included two of our *Oreobates* samples collected in lowland rainforest at Panguana, central Peru. Unexpectedly, in the phylogenetic tree (Fig. 1), these two samples from the same locality were recovered as belonging to two distant clades, namely a clade containing *O. quixensis* from Ecuador and another clade containing *O. saxatilis* from southern Peru. This prompted us to calculate a tree including all 16S sequences from Panguana specimens collected by us plus all those from GenBank identified as *O. quixensis* and *O. saxatilis*.

The resulting phylogenetic tree (Fig. 7) is in agreement with our first analysis and recovered these lowland sam-

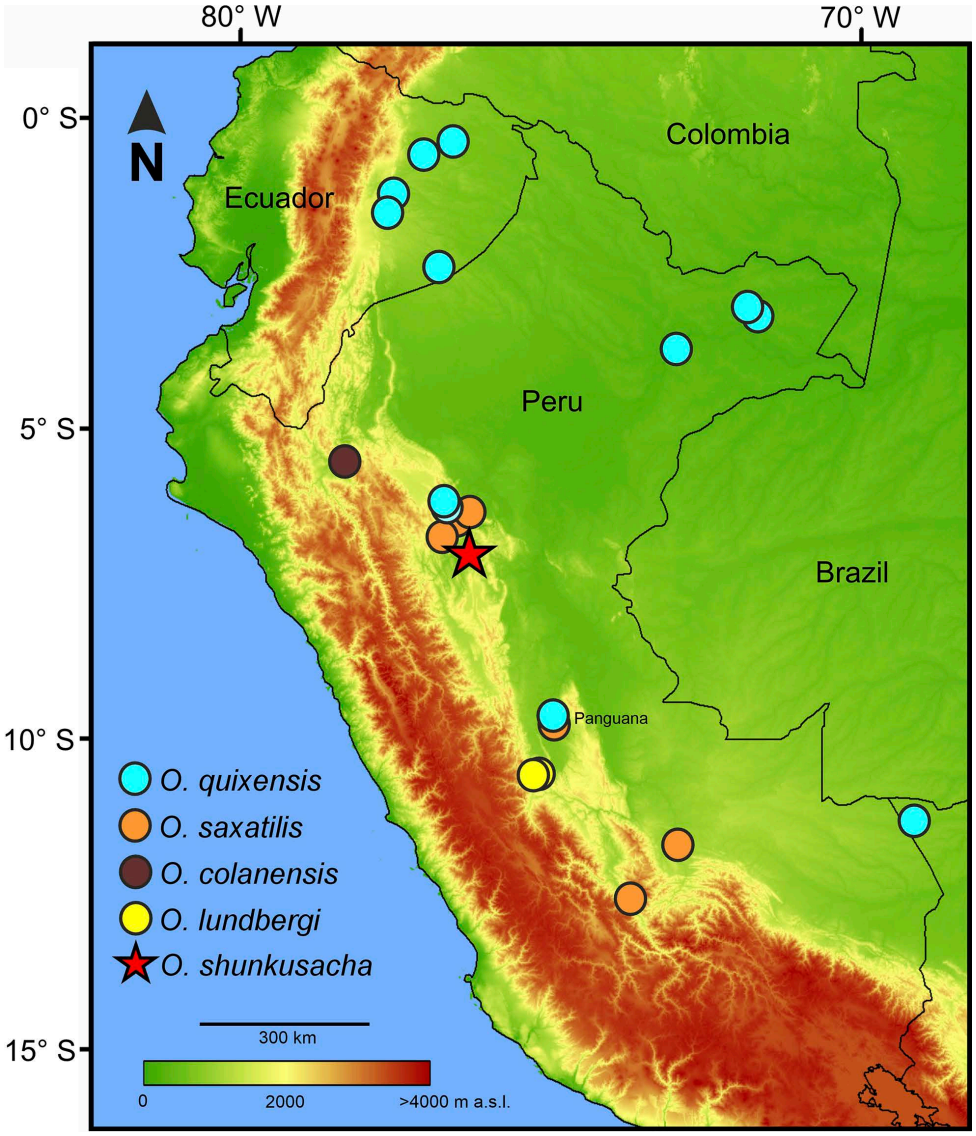

Figure 5. Map of western South America indicating the localities of selected *Oreobates* samples used in our molecular analyses and referred to in the text.

ples in two major clades, being sister to each other with high support (bootstrap/ SH-aLRT values = 100/100). One clade is referable to *O. saxatilis*, including all GenBank sequences identified as such, and the other clade is referable to *O. quixensis*, including GenBank sequences identified as such from Ecuador (type locality of *O. quixensis* in Provincia Napo, Ecuador; Padial et al. 2008), Bolivia and Peru. Samples from Panguana are represented in both of these clades. Uncorrected p-distances between these two clades range between 6.7–10.1%.

As in former analyses (Padial et al. 2012, Montero-Mendieta et al. 2021), the nominal species *O. quixensis* and *O. saxatilis* are recovered paraphyletic, as two samples identified as *O. saxatilis* cluster with all the *O. quixensis* samples (Fig. 7). Remarkably, one of these sequences (EU186708) represents the paratopotype of *O. saxatilis* (KU 212327). Because of its origin from a type specimen, it is of little surprise that paraphyly caused by sequence EU186708 has puzzled researchers in past studies, and three possible explanations for this pattern have been put forward: (1) introgression, (2) incomplete lineage sorting, and/or (3) misidentification of samples (Padial et al. 2012, Montero-Mendieta et al. 2021).

Our data on sympatric (possibly even syntopic) specimens of both clades from Panguana shed some light on this question. Firstly, the 16S uncorrected p-distances are 9.1% between Panguana samples of both clades. This is far beyond the proposed 3% point of reference that was empirically determined to usually characterize distinct species lineages (Fouquet et al. 2007), making it unlikely that these sequences represent intraspecific variation. Secondly, analyses of two nuclear-encoded genes (POMC, RAG-1) revealed a full concordance with the mitochondrial clustering, without nuclear alleles shared between the mitochondrial lineages (Fig. 7).

Examination of the morphology of the Panguana specimens revealed subtle but constant differences between both lineages: dorsal skin strongly tuberculate with numerous enlarged subconical tubercles versus dorsal skin finely tuberculate with few scattered enlarged rounded warts; belly with dark flecking and markings versus belly immaculate white (Fig. 8).

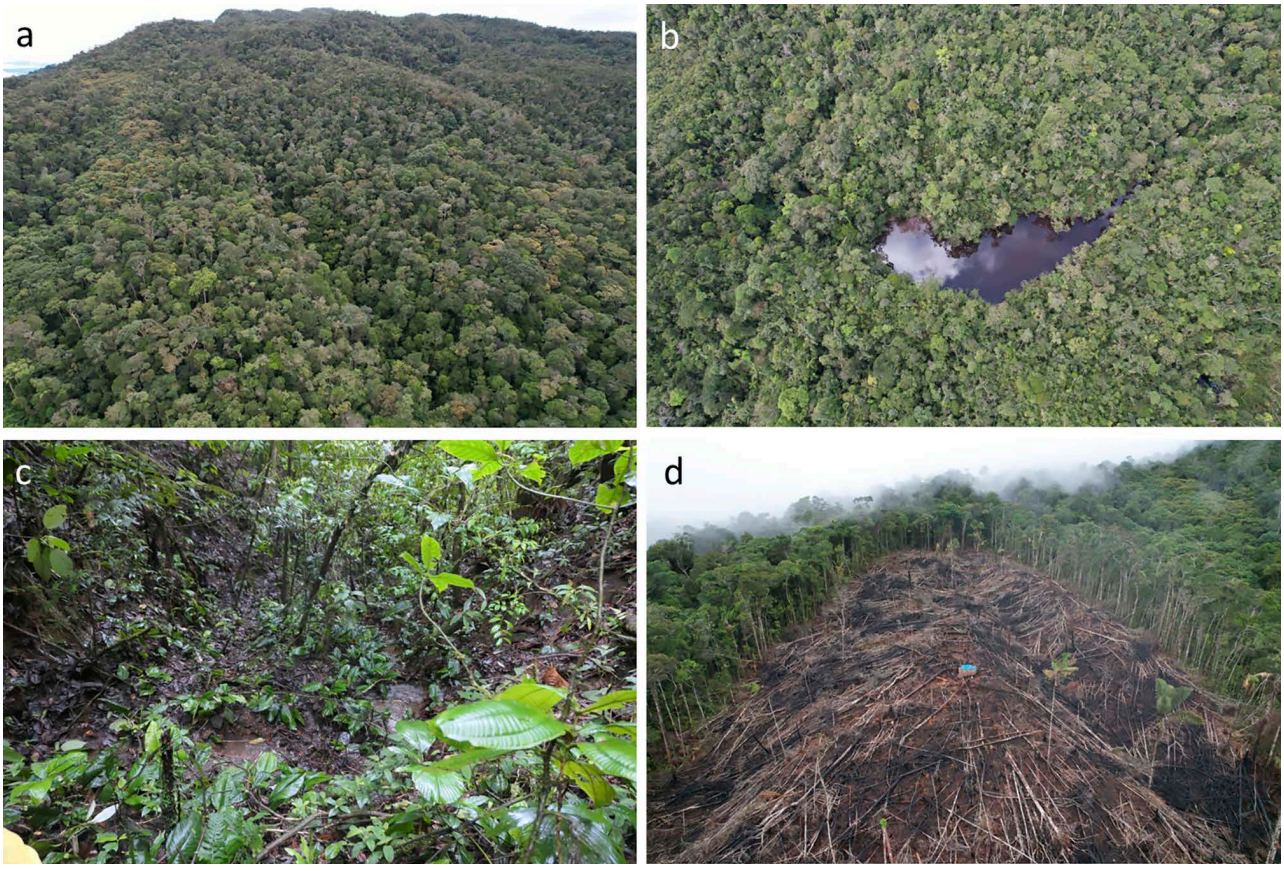

Figure 6. Type locality of *Oreobates shunkusacha* sp. n. within CC Sacha Runa, Sauce District, San Martín Province, San Martín Department, Peru: (a) Landscape view of the montane primary forest at the type locality; (b) aerial view of Lake "Cocha La Encantada" at 1590–1600 m a.s.l.; (c) forest microhabitat with dense undergrowth, a thick layer of leaf litter and roots in sandy and rocky soil, with small surface and underground streams; and (d) 2.5 ha of montane primary forest, which were deforested in November 2024 for the expansion of coffee plots, located about 200 meters from the type locality. Photographed in March 2025 (a, b, d; by D. E. Rado Tipte) and October 2022 (c).

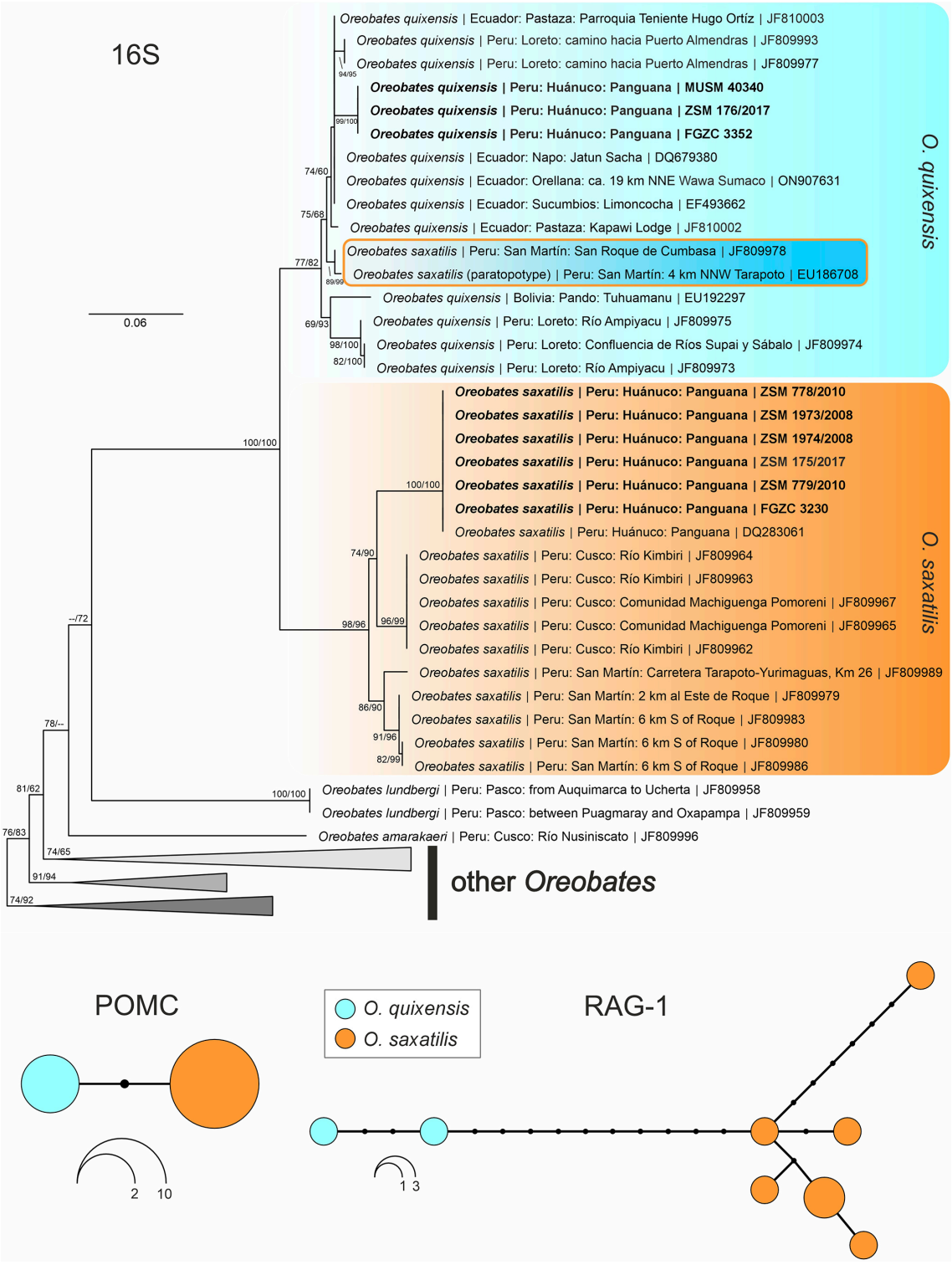

Figure 7. Top: Maximum Likelihood phylogenetic tree of samples of *Oreobates*, here focusing on samples from Amazonian lowlands identified as *O. quixensis* and *O. saxatilis*, inferred from an alignment of the mitochondrial 16S rRNA gene. Numbers at nodes are rounded bootstrap values in percent (2000 pseudoreplicates; not shown if < 50%), followed by SH-aLRT values (1000 replicates; not shown if < 50) as calculated with IQ-TREE. The taxon name is followed by sample locality and GenBank accession number, or voucher number for newly produced sequences (terminals in bold font). Two samples of *Lynchius* were used to root the tree (not shown for better graphical presentation). Bottom: Haplotype genealogies of the nuclear-encoded POMC and RAG-1 genes from specimens of *Oreobates* occurring in sympatry at Panguana (based on phased alleles). Size of circles represents number of times the allele was observed.

Given our results, namely presence of two highly divergent mitochondrial lineages, congruent with differences in two nuclear-encoded genes and with morphological differences, we conclude that two clearly separated, non-admixing species of *Oreobates* occur in close sympatry in the lowland Amazonian forest of Panguana. The one with immaculate belly and rounded dorsal warts is referable to *O. saxatilis* (see Duellman 1990, Padial et al. 2008, Duellman & Lehr 2009), whereas the one with marked belly and subconical tubercles on dorsum is referable to *O. quixensis* (see Padial et al. 2008, Duellman & Lehr 2009), with the respective Panguana samples clustering in the phylogenetic tree with those from Jatun Sacha, Napo, Ecuador, a locality purportedly very close to the type locality of *O. quixensis* (see Padial et al. 2008). As discussed below, these results also suggest misidentifications as the most likely hypothesis to explain the mitochondrial paraphyly of the two taxa.

Discussion

The description of *Oreobates shunkusacha* adds another species to the Yungas-inhabiting *Oreobates*. Among the now 27 recognized nominal species in the genus, the majority (19 species) is known to occur in this type of habitat,

Figure 8. Living individuals of *Oreobates,* corresponding to voucher specimens included in the molecular analyses (Figs 1, 7) and occurring in sympatry at Panguana, Huánuco Department, central Peru, in dorsolateral and ventral views: (a, b) MUSM 40340, *Oreobates quixensis*; (c, d) ZSM 778/2010, *Oreobates saxatilis*. Note differences in dorsal tuberculation and ventral color pattern.

namely humid to semi-humid montane forests at the eastern Andean versant. In contrast, seven species seem to be restricted to lowland habitats (< 700 m a.s.l.), and only one species (*O. ayacucho*) occurs in cold high-Andean Puna grasslands (Padial et al. 2012, Vaz-Silva et al. 2018, Pansonato et al. 2020, Venegas et al. 2021). Apart from several candidate species that have already been characterized (Padial et al. 2012), numerous field expeditions to montane forest habitats in Peru during the last ten years discovered more populations and accumulated more specimens of *Oreobates*, several of which can be expected to represent undescribed species (J. C. Chaparro, pers. comm.). Despite the growing knowledge in *Oreobates* taxonomy, the understanding of the phylogenetic relationships, distribution patterns, biology and threats in this genus remain very limited (Padial et al. 2012, Köhler & Padial 2016, Montero-Mendieta et al. 2021).

Poor knowledge of *Oreobates* frogs is also illustrated by our recent discovery of the sympatric occurrence of two rather common lowland species, *O. quixensis* and *O. saxatilis*, at Panguana in central Peru. Formerly, both species were suggested to occur parapatrically in the upper Amazon basin (Duellman 1990, Duellman & Lehr 2009, Padial et al. 2012). This assumption appears to be the result of very limited data available at that time, as our analysis revealed that both species are relatively widespread, and that some localities for one of the species are in close geographical proximity to localities of the other species, indicating potential partial overlap of the species' ranges in the upper Amazon basin of Peru. Herein, we have provided evidence that two species-level lineages (9.1% uncorrected p-distance in 16S, lack of haplotype sharing in studied nuclear genes, congruent morphological differentiation) occur in sympatry (even in syntopy) in the lowland rainforest of Panguana. These two lineages are allocatable to *O. quixensis* and *O. saxatilis*, respectively.

However, as in former phylogenetic analyses, we also found *O. quixensis* and *O. saxatilis* to be paraphyletic (Figs 1, 7). This paraphyly is caused by two samples identified as *O. saxatilis*, but clustering with samples of *O. quixensis* (see Padial et al. 2012, Montero-Mendieta et al. 2021). At first glance, this paraphyly appeared well-supported given that one of the affected samples originates from the paratopotype (KU 212327) of *Ischnocnema saxatilis* (= *Oreobates saxatilis*) collected together with the holotype (see Duellman 1990). This would, a priori, suggest that misidentification is unlikely. Because the two nominal species are reciprocally diagnosable morphologically, Padial et al. (2012) mentioned the alternative hypotheses of introgressive hybridization or incomplete lineage sorting as a potential reason for paraphyly in mtDNA genealogies. Later, Montero-Mendieta et al. (2021), in a phylogenomic analysis, found *O. saxatilis* and *O. quixensis* consistently paraphyletic in all their analyses, although results consistently proposed two divergent clusters (not congruent with the nominal species). These authors discussed incorrect identification of voucher specimens as one potential reason and, based on their multi-locus data which always resulted in similar topologies independent of the method applied, considered incomplete lineage sorting very unlikely or, at least, of almost no effect. Although our data set is rather limited, we detected no haplotype sharing in nuclear genes between the two lineages occurring at Panguana, and therefore conclude that based on the available knowledge, introgression does not provide a plausible explanation for the paraphyly in mtDNA genealogies.

Misidentification of collected specimens, even by experts, is a frequent problem, particularly if little is known about intra-specific variation, or when morphologically cryptic lineages or juveniles are involved. This phenomenon has also become evident in several cases for type series collected prior to the era of DNA barcoding, which later turned out to contain specimens of different nominal taxa (see e.g., Morales & Icochea 2000, Araujo-Vieira et al. 2023). Furthermore, some characters in preserved specimens may vary with the methodology applied for fixation and preservation. For example, skin texture and distinctness of dermal granules, warts and tubercles often appear differently expressed when compared between specimens of the same species fixed in ethanol versus formalin. Such effects may further contribute to less easily detectable differences in preserved specimens.

The paratype KU 212327 of *O. saxatilis*, namely the voucher specimen of the 16S sequence with the GenBank accession number EU186708 clustering with *O. quixensis* in phylogenetic trees (Padial et al. 2012, Montero-Mendieta et al. 2021, results herein), was collected together with the holotype (KU 212556) by John J. Wiens on 7 February 1989 at Ponga de Shilcayo, 4 km NNW of Tarapoto, in San Martín Department, Peru (Duellman 1990). Examination of photographs of this comparatively broad-headed paratype specimen revealed a relatively strongly tuberculate dorsum with dense scattering of enlarged subconical tubercles, as well as a belly with some sparse dark flecking (Fig. 9). With these character states, the paratopotype differs from the holotype KU 212556, which we examined and was adequately described by Duellman (1990). The holotype (Fig. 9; color photograph of the living holotype provided by Duellman & Lehr 2009: 103) exhibits a finely tuberculate skin on dorsum, with only a few scattered larger tubercles, especially in the scapular region. Its belly is immaculate white.

Padial et al. (2012) mentioned that both species (*O. saxatilis* and *O. quixensis*) are reciprocally diagnosable by morphology, with Padial et al. (2008) and Duellman & Lehr (2009) listing the immaculate belly and the fine dorsal tuberculation with few scattered larger tubercles as key characters of *O. saxatilis*, distinguishing it from *O. quixensis* (belly with dark markings, dorsum with many enlarged subconical tubercles). However, knowledge about intra-specific variation of these characters is very limited and the *O. saxatilis* paratopotype KU 212327 exhibits some intermediate character in belly coloration, namely a white belly with few scattered dark spots and flecks (in contrast to a fully mottled belly). Therefore, we suppose that, al-

though most specimens might be diagnosable by morphology alone, there might be more 'problematic' individuals exhibiting less clear character states and are, therefore, less easy to differentiate. This hypothesis is somewhat supported by the fact that among the genotyped *O. saxatilis* specimen from Panguana, all exhibit an immaculate belly as described for *O. saxatilis*; however, three specimens (ZSM 778–779/2010, ZSM 175/2017) have distinctly dark ventral surfaces of thighs (see Fig. 8), whereas two (ZSM 1973–1974/2008) have immaculate white ventral surfaces of thighs, as in the *O. saxatilis* holotype (Fig. 9). Moreover, the new species *O. shunkusacha* exemplifies that there might be considerable variation in the color pattern of the belly in *Oreobates* (see above), and sexual dimorphism in such color patterns might also be of relevance.

Despite, or because of, this very limited knowledge, we cannot rule out the possibility that the *O. saxatilis* paratopotype KU 212327, judging from its external morphology, could represent a misidentified specimen of *O. quixensis*. Given that, presumably, the jointly collected holotype and paratopotype of *O. quixensis* were fixed and preserved using the same methodology and liquids, dependency of observed differences in dorsal skin texture on different preservation methods can be excluded. For this reason, the different skin textures and ventral color patterns observed among the holotype and the paratopotype of *O. saxatilis* leads us to propose that a misidentification of the paratopotype is likely.

Although fraught with some uncertainty, our assumption of a misidentified *O. quixensis* and its confusion with

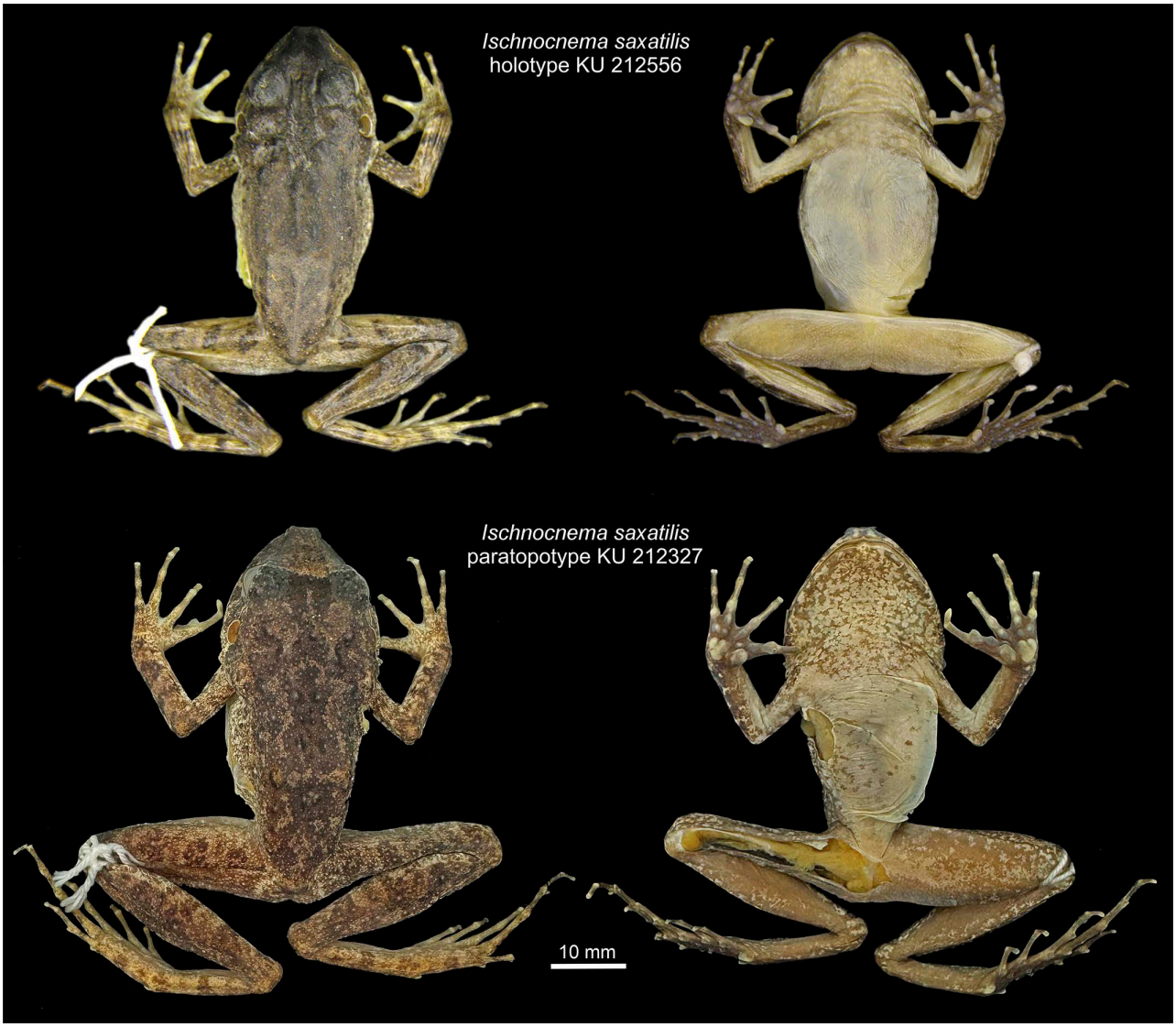

Figure 9. Preserved holotype and paratopotype of *Ischnocnema saxatilis* Duellman, 1990 (= *Oreobates saxatilis*) in dorsal (left column) and ventral (right column) views. The paratopotype KU 212327 is the voucher specimen of the 16S sequence with the GenBank accession number EU186708 and probably referable to *Oreobates quixensis* (see Discussion). Photographs by J. M. Padial and A. P. Motta.

O. saxatilis in its respective type series appears to be the most parsimonious conclusion to explain paraphyly in phylogenetic studies. The same is tentatively assumed for the second *O. saxatilis* sequence clustering with *O. quixensis* and originating from specimen MUBI 9200 (San Roque de Cumbasa, San Martín, Peru). Unfortunately, attempts to find this specimen in the collection to examine its morphological characters have failed thus far (J. C. Chaparro, pers. comm.). Apart from misidentification of specimens, confusion or contamination of samples in the laboratory during DNA extraction could also explain phylogenetic results, but we consider the latter scenario less likely.

Upon correction of these putative misidentified specimens used for sequencing, the resulting phylogeny would be very clear in revealing two monophyletic clusters, one corresponding to *O. quixensis* and the other corresponding to *O. saxatilis*, with close sympatry of both species proven for the locality Panguana (Fig. 7). As is obvious from the mapping of localities included in the genetic sampling (Fig. 5), as well as preliminary barcoding results of samples from lower elevations in the Biocorredor Bosques de Vaquero 'Shunku Sacha' (see above), individuals of both clades occur in close geographical proximity in the San Martín Department, Peru, and probably occur sympatrically at additional localities, including the type locality of *O. saxatilis*, if our assumptions are correct. Such distribution patterns of divergent but closely related sister species exhibiting overlapping ranges and occurring in sympatry at certain localities in lowland Amazonia is not unusual and has recently been documented for another sister pair of pristimantine frogs, *Pristimantis asimus* and *P. reichlei* (Köhler et al. 2024).

Together with former studies, our investigation exemplifies that we are still at the beginning regarding the understanding of the diversity of *Oreobates* frogs. Additional fieldwork, broader sampling, and more comprehensive genetic data are needed to enhance the knowledge of *Oreobates* systematics, their morphological variation, their biology and potential threats.

Acknowledgements

Many thanks to C. Aguilar-Puntriano (MUSM) who generously supported the work of our team in multiple ways. For sharing data, photographs of specimens and miscellaneous support, we thank J. C. Chaparro (MUBI) and J. M. Padial (Universidad Granada). J. Aparicio† (CBF), W. Böhme (ZFMK), B. T. Clark (BMNH), W. E. Duellman† and L. Trueb (KU) kindly provided access to the collection under their care. A. P. Motta (KU) kindly took the photographs of the *O. saxatilis* paratype and provided valuable comments on the manuscript. We thank H. G. Chanchari, Y. Trigoso García, F. Reategui Ramirez, E. R. García, V. Arce Sangama, A. del Aguila Ushiñahua, and M. Arce Chistama, members of the Asociación Ecológica Sacha Runa Sauce (AESARUSA), and C. Zumba Tananta, C. Gatica Rengifo, B. Shapiama Apagueño, J. P. Shapiama Zumba, S. Alvarez Garcia, P. Shapiama Zumba, members of the Asociación Agro Bio Agroforestal Yaku Kawsanapa (ABAFYK), who actively participated in fieldwork and collaborated in this project. We are grateful and acknowledge their important work in voluntarily conserving and managing the forests of the CC Sacha Runa and the CC Yaku Kawsanapa, as we recognize their valuable contributions to this research, and the importance of their local and traditional knowledge, which they willingly integrated through the participatory science methods we jointly applied. Thanks to R. Vilca Lucana, J. Fachin Ruiz, and the entire AMPA Perú team for their valuable contribution to fieldwork organization, and C. Aubert from Nature Conserv'Action for his key contribution to the funding and implementation of our field research. Thanks to K. Bravo Leyva for supervising logistics and planning together with D. E. Rado Tipte, who also provided drone photography and maps, and estimated the geographic range of *O. shunkusacha*. We thank D. A. Barrera Moscoso and C. A. Ramirez Peralta for their assistance with administrative and permit application procedures. We are also grateful to A. Wong, O. Machuca, D. Olivera (members of Ararankha: Ecología y Conservación), and J. C. Cusi for their support with sample and specimen processing, and to L. Flechtner, J. Horz, G. Keunecke, and L. Rothe for their support with laboratory work. For help during fieldwork in 2025, we thank M. Fernandez, M. Valle, T. and Vasquez. Fieldwork in the Biocorredor Bosques de Vaquero 'Shunku Sacha' was conducted under the research and collection permits of SERFOR (RDG N° D000136-2022-MIDAGRI-SERFORDGGSPFFS-DGSPFS, RDG N° D000079-2024-MIDAGRI-SERFOR-DGGSPFFS-DGSPFS), and that at ACP Panguana by INRENA (RDG N° 124-2008-INRENA-IFFS-DCB), and SERFOR (RDG N° 007-2014-SERFOR-DGGSPFFS, RDG N° 0406-2017-SERFOR-DGGSPFFS). Fieldwork in 2022 was funded by Nature Conserv'Action, and by Amazónicos por la Amazonía – AMPA Perú through the project "Ecoturismo científico y comunitario en el biocorredor de concesiones para conservación Cordillera Vaquero – Yaku Kawsanapa – Sacha Runa. Zona de amortiguamiento del Parque Nacional Cordillera Azul y el Área de Conservación Regional Cordillera Escalera, Región San Martín", funded by the Spanish cooperation agency AECID Perú. Fieldwork in 2025 was led by Nature Conserv'Action and Ararankha: Ecología y Conservación, through the project "Co-exist: equitable partnerships and communities in action for the biodiversity of the Biocorridor Bosques de Vaquero in the Andean Amazon"; supported by the Support Programme for biodiversity Civil Society Organisations active in developing countries (ProBioDev) managed by the IUCN French Committee, and funded by the French development agency (AFD), Audemars Piguet Foundation for Trees, Fondation de France, Fondation Manthano, Fondation Egis, and Maisons du Monde Foundation; and also supported by funding from the fonds de dotation Le Poids du Vivant.

References

Altschul, S. F., W. Gish, W. Miller, E. W. Myers & D. J. Lipman (1990): Basiclocal alignment search tool. – Journal of Molecular Biology, **215**: 403–410.

Araujo-Vieira, K., A. C. C. Lourenço, J. V. A. Lacerda, M. L. Lyra, B. L. Blotto, S. R. Ron, D. Baldo, M. O. Pereyra, A. M. Suárez-Mayorga, D. Baêta, R. Barbosa Ferreira, C. L. Barrio-Amorós, C. Borteiro, R. A. Brandão, C. A. Brasileiro, M. A. Donnelly, M. J. M. Dubeux, J. Köhler, F. Kolenc, F. Sá Fortes Leite, N. M. Maciel, I. Nunes, V. G. D. Orrico, P. Peloso, T. L. Pezzuti, S. Reichle, F. J. M. Rojas-Runjaic, H. R. Da Silva, M. J. Sturaro, J. A. Langone, P. C. A. Garcia, M. Trefaut Rodrigues, D. R. Frost, W. C. Wheeler, T. Grant, J. P. Pombal Jr., C. F. B. Haddad

& J. Faivovich (2023): Treefrog diversity in the Neotropics: Phylogenetic relationships of Scinaxini (Anura: Hylidae: Hylinae). – South American Journal of Herpetology, **26** (special issue): 1–143.

Brown, J. L. & E. Twomey (2009): Complicated histories: three new species of poison frogs of the genus *Ameerega* (Anura: Dendrobatidae) from north-central Peru. – Zootaxa, **2049**: 1–38.

Castillo-Urbina, E., F. Glaw, C. Aguilar-Puntriano, M. Vences & J. Köhler (2021): Genetic and morphological evidence reveal another new toad of the *Rhinella festae* species group (Anura: Bufonidae) from the Cordillera Azul in central Peru. – Salamandra, **57**: 181–195.

Castillo-Urbina, E., M. Vences, C. Aguilar-Puntriano, F. Glaw & J. Köhler (2023): Contributing to the taxonomic inventory of green-colored rain frogs: A new species of the *Pristimantis lacrimosus* group (Anura: Strabomantidae) from the southern Cordillera Azul, central Peru. – Vertebrate Zoology, **73**: 1047–1061.

Chávez, G. & R. Puerta (2024): Patrones de fragmentación en las zonas de amortiguamiento de las Áreas Naturales Protegidas en la región San Martín, Perú. – The Biologist, **22**: 253–263.

Chiari, Y., M. Vences, D. R. Vieites, F. Rabemananjara, P. Bora, O. Ramilijaona Ravoahangimalala & A. Meyer (2004): New evidence for parallel evolution of colour patterns in Malagasy poison frogs (*Mantella*). – Molecular Ecology, **13**: 3763–3774.

Cusi, J. C., L. A. G. Gagliardi-Urrutia, I. C. Brcko, D. B. Wake & R. von May (2020): Taxonomic status of the Neotropical salamanders *Bolitoglossa altamazonica* and *Bolitoglossa peruviana* (Amphibia: Caudata: Plethodontidae), with the description of a new species from northern Peru. – Zootaxa, **4834**: 365–406.

Cusi, J. C., J. Moravec, E. Lehr & V. Gvoždík (2017): A new species of semiarboreal toad of the *Rhinella festae* group (Anura, Bufonidae) from the Cordillera Azul National Park, Peru. – ZooKeys, **673**: 21–47.

Duellman, W. E. (1990): A new species of leptodactylid frog, genus *Ischnocnema*, from Peru. – Occasional Papers of the Musuem of Natural History, University of Kansas, **138**: 1–7.

Duellman, W. E. & E. Lehr (2009): Terrestrial-breeding frogs (Strabomantidae) in Peru. – Natur und Tier Verlag, Münster.

Duellman, W. E. & R. Schulte (1993): New species of centrolenid frogs from northern Peru. – Occasional Papers of the Musuem of Natural History, University of Kansas, **155**: 1–33.

Flores, G. & R. W. McDiarmid (1989): Two new species of South American *Centrolenella* (Anura: Centrolenidae) related to *C. mariae*. – Herpetologica, **45**: 401–411.

Fouquet, A., A. Gilles, M. Vences, C. Marty, M. Blanc & N. J. Gemmell (2007): Underestimation of species richness in neotropical frogs revealed by mtDNA analyses. – PLoS One, **2**: e1109.

Frost, D. R. (2025): Amphibian Species of the World: an Online Reference. Version 6.2. – Electronic Database accessible at https://amphibiansoftheworld.amnh.org/index.php, accessed 23 June 2025. – American Museum of Natural History, New York, USA

Guindon, S., J.-F. Dufayard, V. Lefort, M. Anisimova, W. Hordijk & O. Gascuel (2010): New algorithms and methods to estimate maximum-likelihood phylogenies: Assessing the performance of PhyML 3.0. – Systematic Biology, **59**: 307–321.

Kalyaanamoorthy, S., B. Q. Minh, T. K. F. Wong, A. Von Haeseler & L. S. Jermiin (2017): ModelFinder: Fast model selection for accurate phylogenetic estimates. – Nature Methods, **14**: 587–589.

Katoh, K. & D. M. Standley (2013): MAFFT multiple sequence alignment software version 7: Improvements in performance and usability. – Molecular Biology and Evolution, **30**: 772–780.

Katoh, K., K. I. Kuma, H. Toh & T. Miyata (2005): MAFFT version 5: Improvement in accuracy of multiple sequence alignment. – Nucleic Acids Research, **33**: 511–518.

Köhler, J. & J. M. Padial (2016): Description and phylogenetic position of a new (singleton) species of *Oreobates* Jiménez de la Espada, 1872 (Anura: Craugastoridae) from the Yungas of Cochabamba, Bolivia. – Annals of Carnegie Museum, **84**: 23–38.

Köhler, J., E. Castillo-Urbina, C. Aguilar-Puntriano, M. Vences & F. Glaw (2022): Rediscovery, redescription and identity of *Pristimantis nebulosus* (Henle, 1992), and description of a new terrestrial-breeding frog from montane rainforests of central Peru (Anura, Strabomantidae). – Zoosystematics and Evolution, **98**: 213–232.

Köhler, J., F. Glaw, C. Aguilar-Puntriano, S. Castroviejo-Fisher, J. C. Chaparro, I. De la Riva, G. Gagliardi-Urrutia, R. Gutiérrez, M. Vences & J. M. Padial (2024): Similar looking sisters: A new sibling species in the *Pristimantis danae* group from the southwestern Amazon basin (Anura: Strabomantidae). – Zoosystematics and Evolution, **100**: 565–582.

Larsson, A. (2014): AliView: A fast and lightweight alignment viewer and editor for large datasets. – Bioinformatics, **30**: 3276–3278.

Lötters, S. (2003): On the systematics of the harlequin frogs (Amphibia: Bufonidae: *Atelopus*) from Amazonia. III: A new, remarkably dimorphic species from the Cordillera Azul, Peru. – Salamandra, **39**: 169–180.

Lötters, S., P. Debold, K. Henle, F. Glaw & M. Kneller (1997): Ein neuer Pfeilgiftfrosch aus der *Epipedobates pictus*-Gruppe vom Osthang der Cordillera Azul in Perú. – Herpetofauna, **110**: 25–34.

Lötters, S., W. Haas, S. Schick & W. Böhme (2002): On the systematics of the harlequin frogs (Amphibia: Bufonidae: *Atelopus*) from Amazonia. I: Description of a new species from the Cordillera Azul, Peru. – Salamandra, **38**: 95–104.

Martin, A. P. (1999): Substitution rates of organelle and nuclear genes in sharks: implicating metabolic rate (again). – Molecular Biology and Evolution, **16**: 996–1002.

Matschiner, M. (2016): Fitchi: Haplotype genealogy graphs based on the Fitch algorithm. – Bioinformatics, **32**: 1250–1252.

McDiarmid, R. W. (1994): Preparing amphibians as scientific specimens. – pp. 289–296 in: Heyer, W. R., M. A. Donnelly, R. W. McDiarmid, L.-A. C. Hayek & M. S. Foster (eds): Measuring and Monitoring Biological Diversity: Standard Methods for Amphibians. – Smithsonian Institution Press, Washington.

Montero-Mendieta, S., I. De la Riva, I. Irisarri, J. A. Leonard, M. T. Webster & C. Vilà (2021): Phylogenomics and evolutionary history of *Oreobates* (Anura: Craugastoridae) Neotropical frogs along elevational gradients. – Molecular Phylogenetics and Evolution, **161**(107167): 1–13.

Morales, V. R. & J. Icochea (2000): Review of the type material of *Eleutherodactylus mendax* and a new record of *Eleutherodactylus bromeliaceus* from Peru. – Journal of Herpetology, **34**: 158–160.

Motta, A. P., J. C. Chaparro, J. P. Pombal, Jr., J. M. Guayasamin, I. De la Riva & J. M. Padial (2016) Molecular phylogenetics and taxonomy of the Andean genus *Lynchius* Hedges, Duellman, and Heinicke, 2008 (Anura: Craugastoridae). – Herpetological Monographs, **30**: 119–142.

Myers, C. W. & J. W. Daly (1979): A name for the poison frog of Cordillera Azul, eastern Peru, with notes on its biology and skin toxins (Dendrobatidae). – American Museum Novitates, **2674**: 1–24.

Padial, J. M., J. C. Chaparro, S. Castroviejo-Fisher, J. M. Guayasamin, E. Lehr, A. J. Delgado C., M. Vaira, M. Teixeira Jr., C. R. Aguayo-Vedia & I. De la Riva (2012): A revision of species diversity in the Neotropical genus *Oreobates* (Anura: Strabomantidae), with the description of three new species from the Amazonian slopes of the Andes. – American Museum Novitates, **3752**: 1–55.

Padial, J. M., J. C. Chaparro & I. De la Riva (2008): Systematics of *Oreobates* and the *Eleutherodactylus discoidalis* species group (Amphibia, Anura), based on two mitochondrial DNA genes and external morphology. – Zoological Journal of the Linnean Society, **152**: 737–773.

Padial, J. M., T. Grant & D. R. Frost (2014): Molecular systematics of terraranas (Anura: Brachycephaloidea) with an assessment of the effects of alignment and optimality criteria. – Zootaxa, **3825**: 1–132.

Palumbi, S. R., A. Martin, S. Romano, W. O. McMillan, L. Stice & G. Grabowski (1991): The Simple Fool's Guide to PCR. Version 2.0. – Privately published, Univ. Hawaii.

Pansonato, A., A. Motta, P. Cacciali, C. F. B. Haddad, C. Strüssmann & M. Jansen (2020): On the identity of species of *Oreobates* (Anura: Craugastoridae) from central South America, with the description of a new species from Bolivia. – Journal of Herpetology, **54**: 393–412.

Pyron, R. A. & J. J. Wiens (2011): A large-scale phylogeny of Amphibia including over 2800 species, and a revised classification of extant frogs, salamanders, and caecilians. – Molecular Phylogenetics and Evolution, **61**: 543–583.

Rakotoarison, A., A. Crottini, J. Müller, M.-O. Rödel, F. Glaw & M. Vences (2015): Revision and phylogeny of narrow-mouthed treefrogs (*Cophyla*) from northern Madagascar: integration of molecular, osteological, and bioacoustic data reveals three new species. – Zootaxa, **3937**: 61–89.

Salzburger, W., G. B. Ewing & A. von Haeseler (2011): The performance of phylogenetic algorithms in estimating haplotype genealogies with migration. – Molecular Ecology, **20**: 1952–1963.

Shanee, N., S. Shanee & R. H. Horwich (2015): Effectiveness of locally run conservation initiatives in north-east Peru. – Oryx, **49**: 239–247.

Shanee, S., N. Shanee, W. Loc & M. J. Espejo-Uribe (2020): The development and growth of non-governmental conservation in Peru: Privately and communally protected areas. – Human Ecology, **48**: 681–693.

Shimodaira H. & M. Hasegawa (1999): Multiple comparisons of log-likelihoods with applications to phylogenetic inference. – Molecular Biology and Evolution, **16**: 1114–1116.

Stephens, M., N. J. Smith & P. Donnelly (2001): A new statistical method for haplotype reconstruction from population data. – American Journal of Human Genetics, **68**: 978–989.

Tamura K., G. Stecher & S. Kumar (2021): MEGA11: Molecular Evolutionary Genetics Analysis Version 11. – Molecular Biology and Evolution, **38**: 3022–3027.

Trifinopoulos J., L. T. Nguyen, A. von Haeseler & B. Q. Minh (2016): W-IQ-TREE: A fast online phylogenetic tool for maximum likelihood analysis. – Nucleic Acids Research, **44**(W1): W232–W235.

Twomey, E., J. Delia & S. Castroviejo-Fisher (2014): A review of northern Peruvian glassfrogs (Centrolenidae), with the description of four new remarkable species. – Zootaxa, **3851**: 1–87.

Vaz-Silva, W., N. M. Maciel, S. P. de Andrade & R. C. Amaro (2018): A new cryptic species of *Oreobates* (Anura: Craugastoridae) from the seasonally dry tropical forest of central Brazil. – Zootaxa, **4441**: 89–108.

Vences, M., A. Miralles, S. Brouillet, J. Ducasse, A. Fedosov, V. Kharchev, I. Kostadinov, S. Kumari, S. Patmanidis, M. D. Scherz, N. Puillandre & S. S. Renner (2021): iTaxoTools 0.1: Kickstarting a specimen-based software toolkit for taxonomists. – Megataxa, **6**: 77–92.

Vences, M., S. Patmanidis, J.-C. Schmidt, M. Matschiner, A. Miralles & S. S. Renner (2024): Hapsolutely: a user-friendly tool integrating haplotype phasing, network construction and haploweb calculation. – Bioinformatics Advances, **4**: vbae083.

Venegas, P. J., L. A. García-Ayachi, J. Ormeño, S. Bullard, A. Catenazzi & A. P. Motta (2021): Two new species of terrestrial-breeding frogs (Anura: Brachycephaloidea) from Cordillera de Colán, Peru. – Neotropical Biodiversity, **7**: 279–296.

Vieites, D. R., M. S. Min, D. B. Wake (2007): Rapid diversification and dispersal during periods of global warming by plethodontid salamanders. – Proceedings of the National Academy of Sciences of the USA, **104**: 19903–19907.

Supplementary data

The following data are available online:

Supplementary Figure S1. Map of forest cover loss within the Biocorredor Bosques de Vaquero 'Shunku Sacha'.

Appendix
Additional specimens examined

Oreobates choristolemma: BOLIVIA: La Paz: Serranía de Bella Vista, CBF 5611 (holotype).

Oreobates cruralis: BOLIVIA: Cochabamba: El Palmar, 1300 m a.s.l., Parque Nacional Carrasco, ZFMK 72570; between Paractito and El Palmar, ZFMK 66964 ZFMK 66971–66972, ZFMK 72541–72543; Los Guácharos (Chapare, 500 m a.s.l.), ZFMK 72532; La Paz: La Paz (locality in error), BMNH 1947.2.15.70 (holotype); road from Caranavi to Palos Blancos, ZFMK 80599; Santa Cruz: road to Bellavista near road to Samaipata, ZFMK 71997; La Hoyada, 1800 m a.s.l., Parque Nacional Amboró, ZFMK 72644; south of Cuevas, 1100 m a.s.l., ZFMK 72644.

Oreobates discoidalis: ARGENTINA: Tucumán: Horco Molle, "13 km W of Tucumán," Sierra de San Javier, ca. 1200 m a.s.l., BMNH 1947.2.15.63–65 (syntypes).

Oreobates granulosus: PERU: Puno: Santo Domingo, Carabaya, 6000 ft (1800 m a.s.l. aprox.), BMNH 1947.2.15.72 (holotype).

Oreobates ibischi: BOLIVIA: Santa Cruz: km 68.5 on Santa Cruz de la Sierra-Samaipata road, 750 m a.s.l., CBF 3341 (holotype); El Fuerte de Samaipata, 1900 m a.s.l., ZFMK 60402 (paratype).

Oreobates lundbergi: PERU: Pasco: road Puagmaray to Oxapampa km 77, 2550 m a.s.l., MUSM 19321 (paratype), Paucartambo, MUSM 18424 (paratype).

Oreobates pereger: PERU: Ayacucho: Yuraccyacu, Tambo–Valle del Apurímac trail, 2650 m a.s.l., MUSM 13980 (paratype; formerly LSUMZ 26120).

Oreobates quixensis: ECUADOR: Napo: San José de Moti, MNCN 1708 (lectotype; photos only); PERU: Huánuco: Panguana, MUSM 40340, ZSM 176/2017.

Oreobates sanctaecrucis: BOLIVIA: Cochabamba: Karahuasi, 2200 m a.s.l., ZFMK 72647; Santa Cruz: El Chapé, Parque Nacional Amboró, 2060 m a.s.l., MNK-A 1198 (holotype).

Oreobates sanderi: BOLIVIA: La Paz: Colonia Eduardo Avaroa, ca. 30 km north of Caranavi on the road from Caranavi to Yucumo, ZFMK 80600–80601 (paratypes).

Oreobates saxatilis: PERU: San Martín: Pongo de Shilcayo, about 4 km NNW of Tarapoto, 470 m, KU 212556 (holotype), KU 212327 (paratype; photos only); 27 km NE of Tarapoto, MUSM 8431–8432 (paratypes); Huánuco: Panguana, ZSM 1973–1978/2008, ZSM 778–779/2010, ZSM 175/2017.

Oreobates yanucu: BOLIVIA: Cochabamba: old Chapare road, 1500 m a.s.l., ZFMK 72569 (holotype).

Oreobates zongoensis: BOLIVIA: La Paz: Valle de Zongo, 1250 m a.s.l., CBF 2503 (holotype).